



Activities on Si-TPC with GEMs

A. Bamberger¹, K. Desch², A. Fauler³, M. Killenberg², X. Llopart⁴, U. Renz¹, M. Ummerhofer², M. Titov^{1,5}, N. Vlasov^{1,2}, P. Wienemann², S. Zimmermann^{1,2}, A. Zwerger¹

January 08, 2008

Abstract

This memo reports on the progress of the development of a highly pixelated and integrated readout system for a TPC. A triple GEM stack is used for gas amplification. The readout is performed using the TimePix CMOS ASIC developed within the EUDET/SiTPC collaboration. The spatial as well as the time resolution of the GEM-TimePix system are probed in a 5GeV electron test beam at DESY. Furthermore advances in hardware development, achieved in collaboration with CERN and the FMF in Freiburg, are presented.

¹ Albert-Ludwigs University, Freiburg, Germany

² Rheinische Friedrichs-Wilhelms-University, Bonn, Germany

³ Freiburger Material Forschungszentrum, Freiburg, Germany

⁴ CERN, Geneva, Switzerland

⁵ CEA Saclay, DAPNIA/SPP, Gif sur Yvette, France

1 Introduction

The ongoing development of Micro-Pattern-Gas-Detectors allows an extended field of applications for gaseous detectors. In recent years the feasibility of an unconventional readout scheme for such detectors was proven [1,2,3]. This is expected to be employed in future astrophysical and high energy physics experiments, such as the Next Generation X-Ray Telescope (NXGT) [3] or the Time-Projection-Chamber for the proposed International Linear Collider (ILC) [4].

The prospects of this detection concept are investigated in two test beam runs with 5GeV electrons at DESY. In this case the resolution is affected by multiple scattering at a negligible level, as compared with the use of electrons from radioactive sources. A Si-telescope for external tracking provides independent information on the track position. With the new TimePix CMOS readout chip [5] a spatial resolution in the order of 20-25 μ m and a time resolution of better than 10ns are achieved.

2 The test beam setup

2.1 Basic 3GEM and TimePix setup

The basic setup consists of a gas tight aluminium box with very thin entrance and exit windows for the electron beam and a Plexiglas cover for inspection purposes. Inside the box the triple GEM/TimePix stack and analogue L3- μ -amplifiers are housed. A cross-sectional view of the GEM stack with the TimePix is given in Fig. 1. Electrons from the test beam transverse the active volume of 10 \times 10 \times 0.6cm³. The electric field in the drift region is about 1.1kV/cm. Three standard CERN-produced GEMs [6] of the same active surface as the base of the drift volume amplify the electrons from the ionising particles. Their geometrical features are hexagonally arranged holes with a pitch of 140 μ m and of 70 μ m (50 μ m) outer (inner) diameter. The distance between the first, second and third GEM is each 2mm with an applied transfer field of $E_T \approx 3-3.5$ kV/cm. The grounded readout plane beyond the last GEM is exposed to a field of around $E_I = 4$ kV/cm of the induction gap. High fields in the order of ≈ 70 kV/cm are necessary for the gas amplification. They are well confined within the region of the GEM holes. This helps to protect the readout chip against harmful discharges. The necessary potentials are created by a resistor chain near the triple GEM/TimePix stack. With

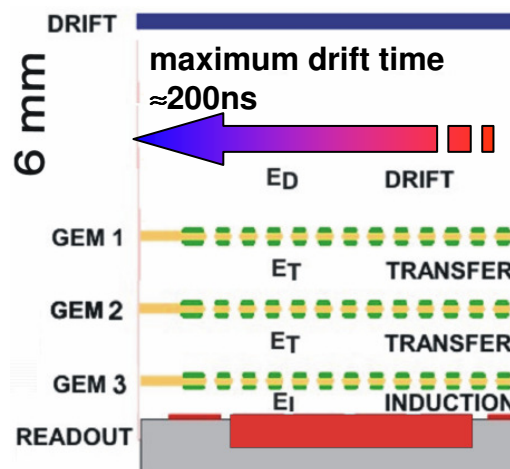


Figure 1: Schematic view of the GEM stack with TimePix. The arrow indicates the electron beam.

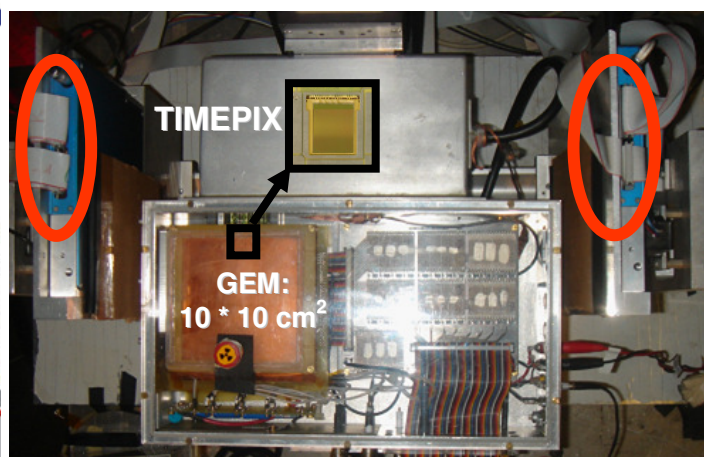


Figure 2: Setup installed in the test beam. Red circle indicate the position of the Si-telescope and the scintillating beam counters.

this configuration a gain in the order of $\approx 10^5$ can be achieved in Ar/CO₂ (70/30) and He/CO₂ (70/30).

In addition to the standard GEMs also a special type of GEMs with holes of 30 μ m outer and \approx 20 μ m inner diameter is tested. The pitch of the holes is 50 μ m. This type of GEMs has first been used by Bellazzini et al [3].

2.2 Test beam setup

The TimePix chip is positioned close to the border of the GEM-stack, see Fig. 2. The remaining part of the anode is covered by a matrix of 24 pads, individually connected to L3- μ -amplifiers. These are used to estimate gas gain and to monitor the GEM operation.

The trigger for the data acquisition is given by the coincidence of scintillating counters, two upstream and crossed in the beam and another counter downstream. A Si-strip telescope consisting of three layers is used to define the position of the beam electrons. In front of the triple GEM/TimePix box there are two crossed planes of Si-strips for a simultaneous measurement of the x-y-coordinate. Another layer behind the box records the y-coordinate of the exiting beam. The pitch between two strips is 50 μ m. The hit multiplicity of the Si telescope is used as first veto to reject double track events.

All I/O operations between PC and TimePix are handled by the MUROS2 board and a National Instrument 6533 DIO-card. A fast shutter gate of fixed length is applied through the MUROS2 to the TimePix. This activates the acquisition mode of the chip and is needed as timing reference.

2.3 TimePix: Time, TOT and Mixed-Mode (MM)

The TimePix is a CMOS pixel ASIC based on the layout of the MediPix2 chip [7] developed by the MediPix collaboration. The EUDET/SiTPC collaboration commissioned a redesign of the original chip to add a time reference. This allows for example the measurement of the drift time, which is important in a TPC.

The TimePix consists of 256 \times 256 pixels of 55 \times 55 μ m² size each, forming a total active surface of 14 \times 14mm². Every single pixel cell has a charge sensitive input and is equipped with amplifying, shaping and discriminating front-end electronics. Signals of positive and negative polarity can be processed. A reference clock is distributed throughout the entire chip. Depending on the chosen mode of operation an on-pixel shift register counts the number of clock cycles. The design value for the clock speed is up to 100MHz. The way of counting depends on the chosen mode of operation. In case of the TIME mode the time of arrival of the charge signal is recorded, which provides the information on the drift time. The Time-Over-Threshold (TOT) mode records the duration of a pulse above the adjustable threshold. This value can be related with the total charge delivered to the input. The MediPix2 mode is inherited from the predecessor of the TimePix. There the number of hits on a pixel is recorded. The dynamic range is limited by the maximum number of counts per shift register namely 11810. A situation in which every other pixel is set to TIME or TOT mode resulting in a checkerboard like pattern is called Mixed-Mode (MM). An image of the TimePix is displayed in the inset of Fig. 2.

3 Event Reconstruction

3.1 Clustering

This investigation uses an event reconstruction, which facilitates the evaluation of track position by clusters originating from the ionisation process in a gas.

When an event is recorded in MM, then half of the pixels record the TOT-information, while the other half of the pixels measures the time. Therefore the first step in an event reconstruction is the mapping of the data separately on two 256×256 pixel grids. An interpolation of the missing TOT or Time pixel entries is performed, using the information from the respective next neighbours. In Fig. 3 a typical event is shown. The left part shows the processed event in TOT mode, the right part in TIME.

Then in a second step the clusters are separated using only the TOT information. An algorithm based on the “island” reconstruction algorithm from the ZEUS calorimeter group [8] is used for this purpose. All pixels are sorted first according to their TOT-value. Then the pixel with the highest count is the seed for the first cluster. Adjacent pixels with non-zero counts are assigned to this cluster. If a pixel is encountered which is not close to any already existing cluster a new one is started. This method yields approximately twice the number of clusters than reported previously in [1,9]. There the clustering is based on contiguous areas of pixels. The increase by about a factor two is a typical number for the data shown; it depends on both, the threshold setting, usually $\approx 10^3 e^-$, and the gas gain as quoted above.

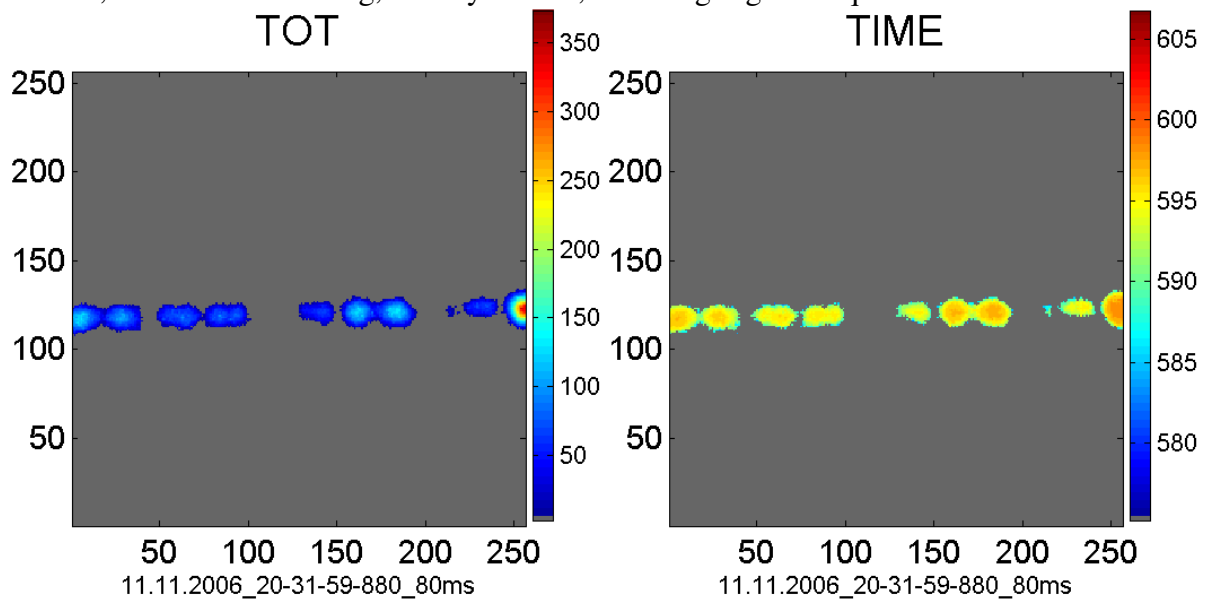


Figure 3: The left part shows the event as recorded in the Time-Over-Threshold mode. At the right the same event is displayed as seen in Time-mode.

3.2 Resolution determination

Typically 11-12 separated clusters are observed per event. A special cut removes double or multi track events from further analysis. The evaluation of the unbiased resolution is discussed in detail in [1]. Two different kinds of straight line fits are performed. The first fit is performed to all N clusters belonging to a track. Then all residuals to the fit for the N points are calculated. In a second fit one cluster is removed and the fit is done on N-1 clusters. For the exempted cluster the residual from the fit is estimated. This is repeated for each of the N clusters. These residuals result in two Gaussian distributions of different standard deviations, σ_N and σ_{N-1} respectively. The geometric mean of both produces a measure for the unbiased resolution $\sigma_{mean} = \sqrt{\sigma_N \times \sigma_{N-1}}$.

There are primarily two contributions to σ_{mean} . First there is the transverse diffusion in the drift space. Second there is the intrinsic resolution limit due to the gas amplification system and the readout scheme (“hardware” limit). This can be parameterized as follows

$$\sigma_{mean} = \sqrt{\underbrace{\sigma_0^2}_{\substack{\text{hardware} \\ \text{"limit"}}}} + \underbrace{D_t^2 \times y / n_{cl}^{el}}_{\substack{\text{transverse} \\ \text{diffusion}}}.$$

Using the information from the telescope the data are sorted into different bins along the drift direction y . For each bin in the drift direction σ_{mean} is determined. A fit to this values yields a σ_0 in the order of 20-30 μm . The corresponding plots for Ar/CO₂ and He/CO₂ are shown in Fig. 4. As expected the resolution as function of y shows a square root dependence.

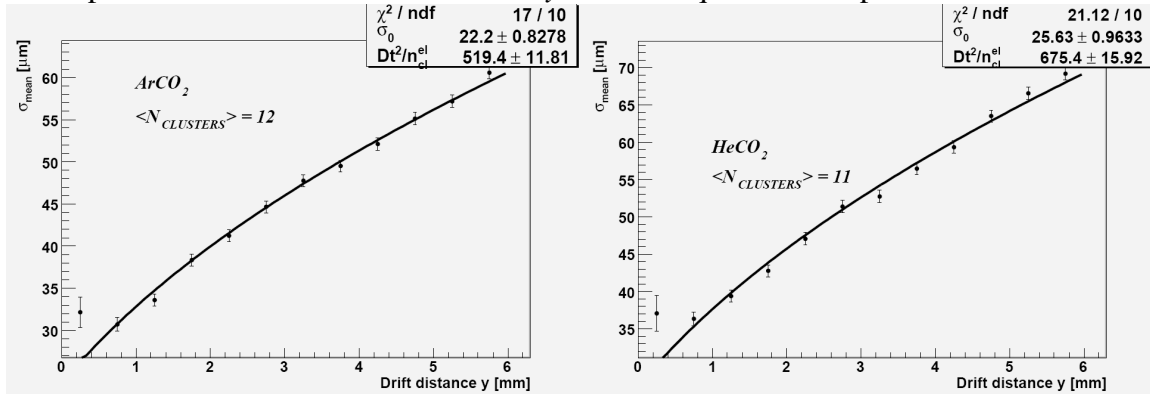


Figure 4: The resolution σ_{mean} as function of the drift distance is shown. The left plot is for Ar/CO₂ (70:30) and the right for He/CO₂ (70:30).

3.3 Time studies

In the latest measurements a clock-frequency of 100MHz is selected. After receiving a trigger from the coincidence of the three beam counters the chip is made sensitive by the fast shutter gate for a fixed time of 100 μs . Upon arrival of a charge on the pad the pixel either counts the TOT of this pulse or the time passed until the end of the 100 μs shutter. From the latter one can derive the drift time and reconstruct the y coordinates of a track.

The correlation of pulse height (\sim TOT) and TIME in the MM-data reveals a non-negligible time walk. In Fig. 5 the correlation of TIME versus TOT for a typical event is shown. For small pulse heights the TIME values are smaller than the asymptotic value, i.e. they are delayed, basically because of a finite rise time of the on-pixel preamplifier. Based on this finding a correction algorithm for the TIME data is developed.

First the TIME at the maximum TOT value near the centroid of each reconstructed cluster is taken and corrected. Then the average over all these TIME values in a single event is determined. Third all deviations to this mean are derived. This is performed for all events in a given bin of drift distance. As displayed in Fig. 6 these deviations form a Gaussian-like distribution, and result in a time resolution of about 10ns.

3.4 Effect of GEM-pitch

In view of the small values of spatial resolution at drift distances close to the first GEM (\approx 20 μm) possible effects of discrete nature as the pitch of the GEM holes and even the finite pitch of the readout has to be considered.

In order to investigate this effect in the present setup a spatial Fast Fourier Transformation (FFT) on the distribution of the centroids from the track fit is performed. For this all y -centroids of tracks near the first GEM from a high statistics run are projected onto the chip x -axis approximately orthogonal to the tracks. The distribution is shown in Fig. 7. Already here a periodic structure is seen. This observation matches the result of the FFT transformation on this data where a signal of $(8.39 \pm 0.04)\text{mm}^{-1}$ spatial frequency is apparent, which corresponds

to a period of $(119.2 \pm 0.6) \mu\text{m}$, shown in Fig. 8. This is in very good agreement with the projected GEM-hole pitch of $120 \mu\text{m}$ in this direction.

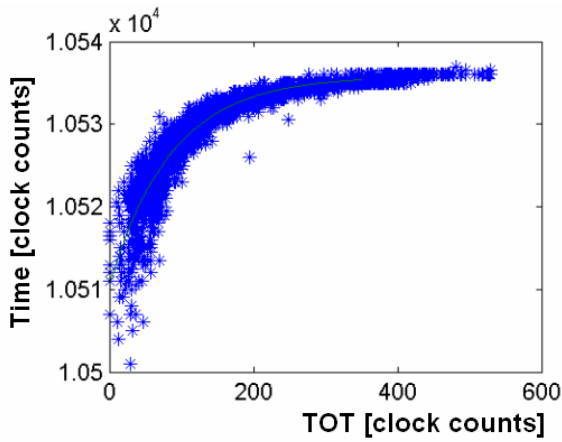


Figure 5: Shown is the correlation of TOT and Time. The clock frequency is 100MHz, which equals 10ns per count.

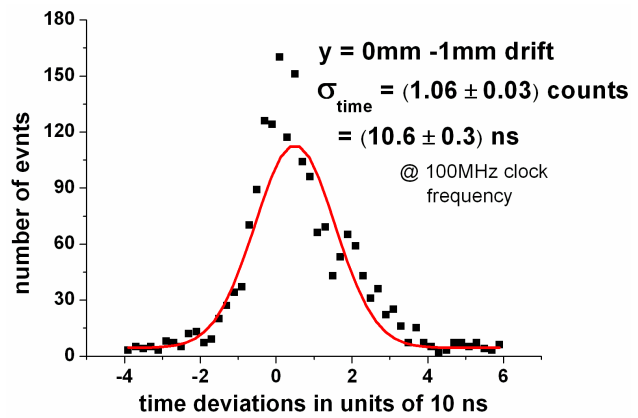


Figure 6: Time value is taken at the maximum TOT in a reconstructed cluster. Then the times in an event are averaged and the deviations from the mean are taken.

Since the GEM is slightly rotated against the coordinate system of the chip, the maximum of the spatial frequency amplitude occurs at an angle of 0.11° . It disappears within a small angular range of $\pm 0.4^\circ$. It is also interesting to note that the signal disappears for large drift distances beyond 1.0mm. Here the averaging due to the transverse diffusion of primary electrons of multi-electron clusters starts to dominate.

A rotation of the GEM by 90° results in a projected pitch along the tracks of $70 \mu\text{m}$, see Fig. 9. In a second measurement with this configuration any periodic structure has vanished, as shown in Fig. 10 and Fig. 11. A scan over the rotation as described above did not reveal any signal that would be expected at a period of $70 \mu\text{m}$.

However notice that the change in σ_0 is not significant. The plot of the resolution as function of y is shown in Fig. 12. The change in σ_0 is $\approx 2 \mu\text{m}$, compared to Fig. 4 (Ar/CO₂). Nevertheless a closer look reveals that the first measured σ_{mean} at $y=0.5\text{mm}$ in this

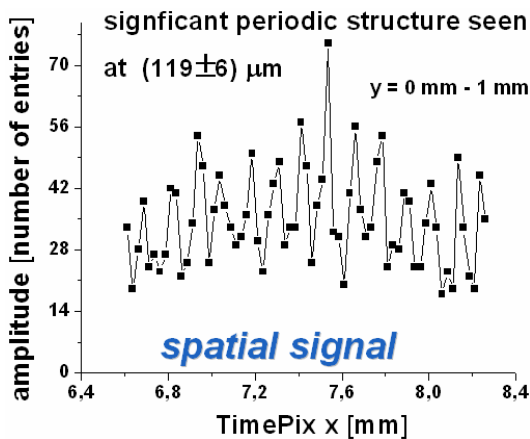


Figure 7: Projected distribution of x-coordinate of calculated cluster centres along the track axis.

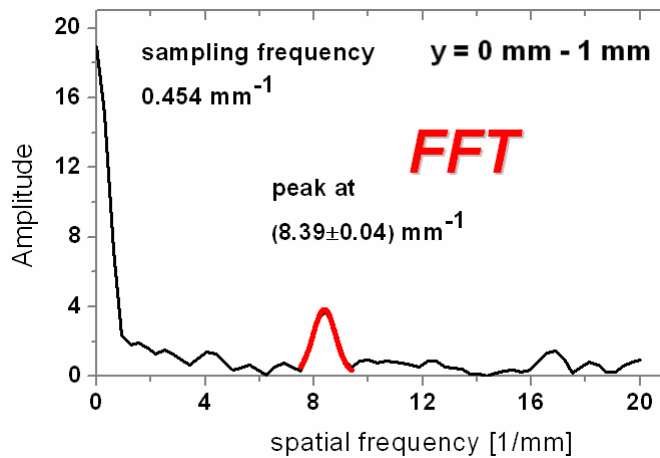


Figure 8: Fast Fourier Transformation of the distribution in Fig. 7.

measurement fits better the expected square root dependence than in the former case where the spatial frequency signal is seen.

One should also note that the effect of a possible discreteness of the centroids affects the deviation from a fitted line only if the track is nearly parallel to the GEM-hole-pattern. The σ would naively be $120\mu\text{m}/2=60\mu\text{m}$, if the electrons passed strictly parallel and in between two rows of holes. The existing angular dispersion of about 1° for the tracks is expected to greatly suppress possible systematic effects.

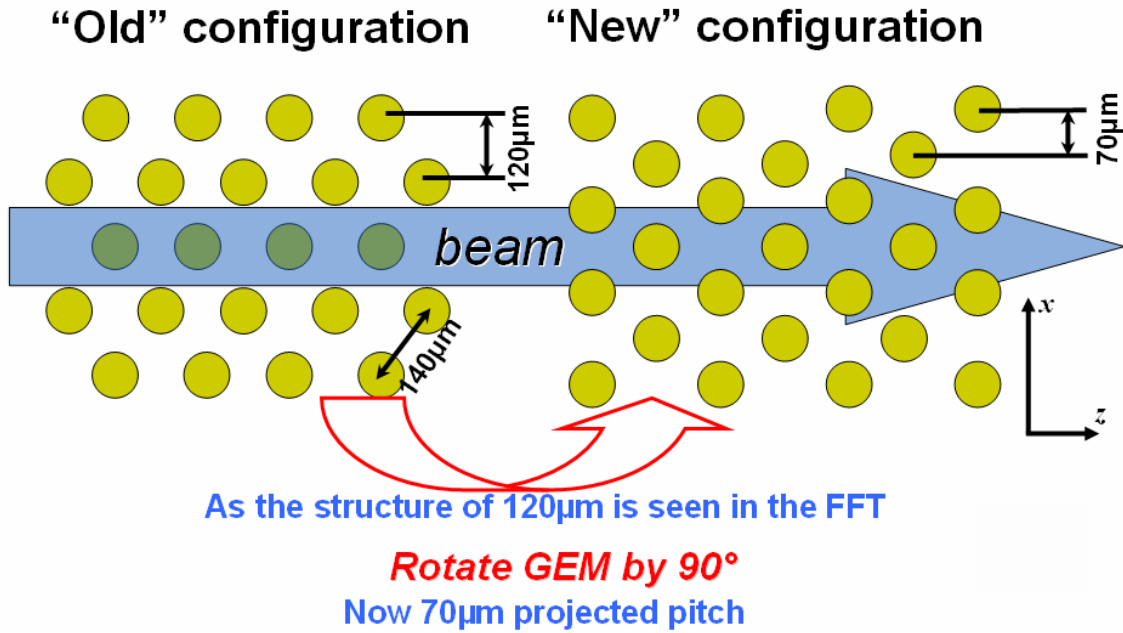


Figure 9: Illustration of the rotation of the GEM hole geometry.

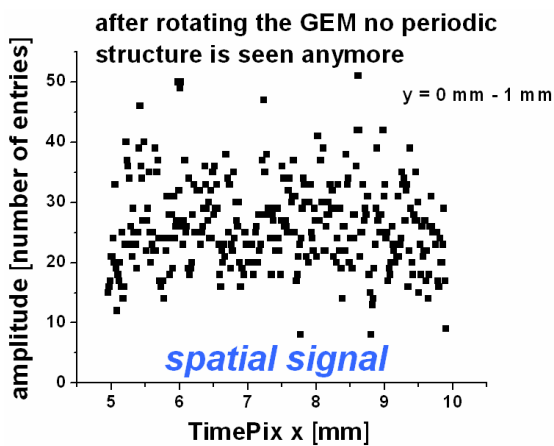


Figure 10: Projected distribution of x-coordinate of calculated cluster centres along the track axis after rotation.

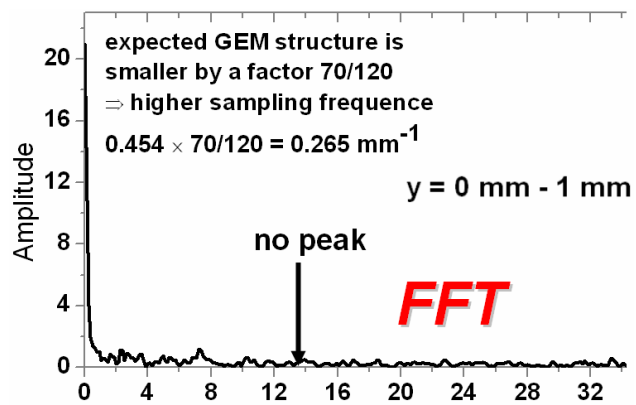


Figure 11: Fast Fourier Transformation of the distribution in Fig. 10.

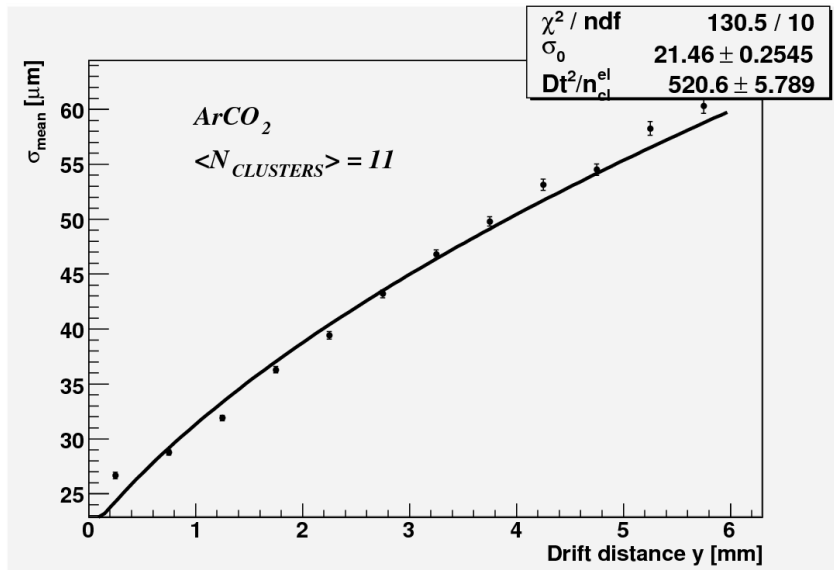


Figure 12: The resolution σ_{mean} as function of the drift distance is shown for ArCO₂ after rotating the GEM.

4 Hardware developments

4.1 New GEM type

In the latest test beam also an unconventional type of GEMs is used. They were developed at CERN for X-ray polarization measurements [3]. Their geometrical features are shown in Fig. 13. The active surface is only $28 \times 24 \text{ mm}^2$, which is surrounded by a guard ring. These GEMs have a hole-pitch of only $50 \mu\text{m}$ and the nominal outer/inner hole diameter is around $30 \mu\text{m}/20 \mu\text{m}$. In order to install them in the existing setup, a special frame is developed for the correct positioning above the TimePix chip, see Fig. 14. In Fig. 15 a schematic view of a stack from three such GEMs is presented.

A gain measurement with this setup for several gases is plotted in Fig. 16. The maximum achievable gain is primarily limited by spurious high density of primary ionisation, as outlined in reference [10]. In less harsh radiation environments than the test beam, e.g. single photo electrons, a significantly higher gain is expected. An improvement of σ_0 by $\approx 6 \mu\text{m}$ is observed compared to the measurements with the standard GEMs, see Fig. 17.

4.2 Pixel enlargement for the MediPix2/TimePix

In collaboration with the Freiburger Material-Forschungszentrum (FMF) a process is developed to enlarge the effective size of a pixel from $55 \times 55 \mu\text{m}^2$ to $110 \times 110 \mu\text{m}^2$. For the time being this process is only tested on a MediPix2 chip, but can easily be applied to a TimePix after studying the properties of this new design.

The advantage of a larger pixel surface is the increase of area where charge is collected. This might reduce the effective threshold of the detector. Therefore it is expected that the system can be operated at a lower gas gain or at a higher efficiency for single electron clusters. A picture of the modified and the original chip is shown in Fig. 18.

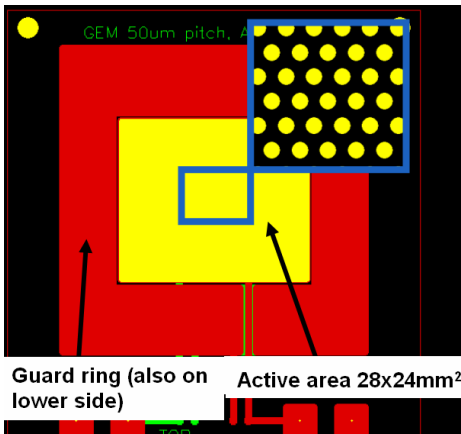


Figure 13: Schematic of a small pitched GEM. The blue rectangle shows magnified a part of the active area.

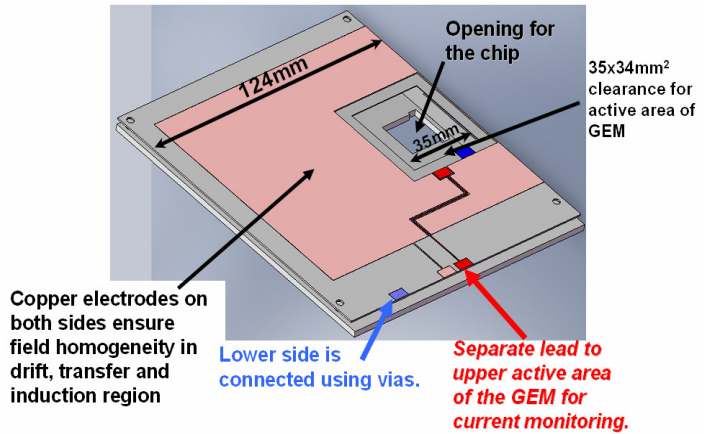


Figure 14: Fixation for the small GEM foil.

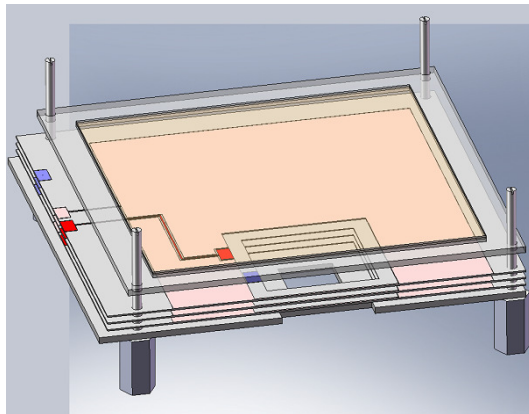


Figure 15: Schematic view of triple GEM stack for the small pitched GEMs.

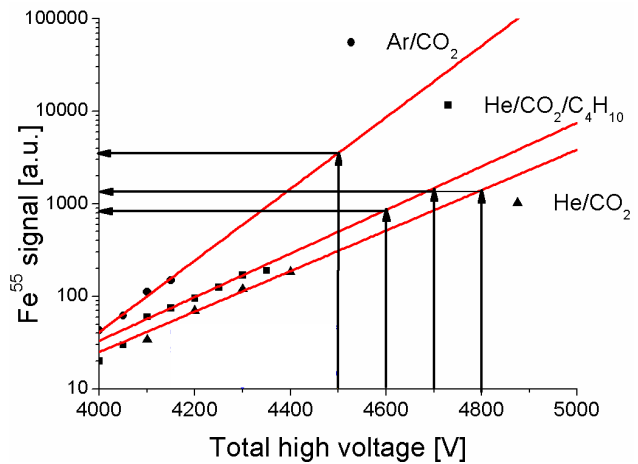


Figure 16: Relative gain comparison for the small GEMs.

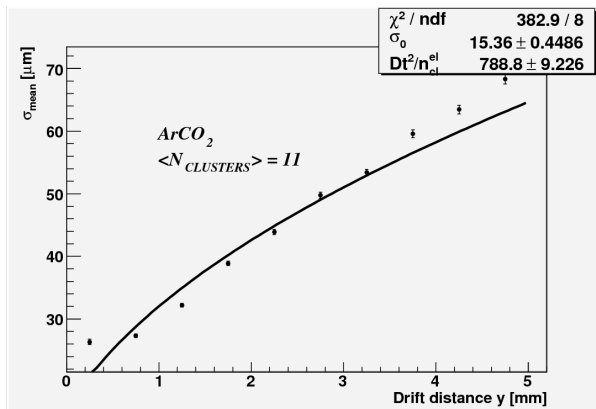


Figure 17: The resolution σ_{mean} as function of the drift distance is shown in ArCO₂ for a small pitched GEM.

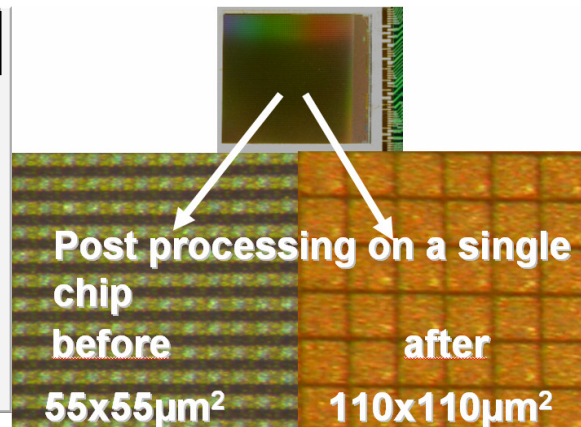


Figure 18: The MediPix2 chip left before and right after post processing.

5 Conclusion

In the recent second test beam at DESY the first results from November 2006 have been validated. A resolution of $\sigma_\theta = 20\text{-}30\mu\text{m}$ in space and of about 10ns in time are feasible with this triple GEM/TimePix TPC-readout prototype using the standard CERN GEMs. GEMs with a smaller hole-pitch of $50\mu\text{m}$ show an even better σ_θ of $\approx 15\mu\text{m}$.

The development of a post processing technology to enlarge the size of the pixel cells from $55\times 55\mu\text{m}^2$ to $110\times 110\mu\text{m}^2$ promises to reduce the effective threshold of the setup.

Acknowledgement

This work is supported by the Commission of the European Communities under the 6th Framework Programme “Structuring the European Research Area”, contract number RII3-026126.

We thank the FMF and the MediPix collaboration for providing us with readout software and hardware. We would also like to thank Michael Campbell, Rui De Oliveira, Erik Hejne, Xavier Llopart and Fabio Sauli for stimulating discussion and valuable advices.

References

- [1] A. Bamberger et al., “Readout of GEM Detectors Using the Medipix2 CMOS Pixel Chip”, Nucl. Instr. Meth. A581 (2007) p.274
- [2] M. Campbell et al., “The detection of single electrons by means of a Micromegas-covered MediPix2 pixel CMOS readout circuit”, Nucl. Instr. Meth. A540 (2005) p.295
- [3] R. Bellazzini et al., “Reading a GEM with a VLSI pixel ASIC used as a direct charge collecting anode”, Nucl. Instr. Meth. A535 (2004) p.477
- [4] T. Behnke et al., “TELSA TDR volume IV: A Detector for TESLA”, DESY 2001-011, ECFA 2001-209
- [5] X. Llopart, “TimePix, a 65k programmable pixel readout chip for arrival time, energy and/or photon counting measurements”, Nucl. Instr. Meth. A581 (2007) p.485
- [6] F. Sauli, “A new concept for electron amplification in gas detectors”, Nucl. Instr. Meth. A386 (1997) p.531
- [7] M. Campbell et al., “Medipix2: a 64-k Pixel Readout Chip With 55-mm Square Elements Working in Single Photon Counting Mode”, IEEE Trans. Nucl. Sci., Vol. 49 (2002) NO. 5
- [8] <http://www-zeus.desy.de/components/fclr/>
- [9] A. Bamberger et al., “Readout of GEM Detectors Using the MediPix2 Chip”, Nucl. Instr. Meth. A573 (2007) p.361
- [10] S. Bachmann et al., “Discharge studies and prevention in the gas electron multiplier (GEM)”, Nucl. Instr. Meth. A479 (2002) p.294